1521-0103/361/3/441–453$25.00
THE JOURNAL OF PHARMACOLOGY AND EXPERIMENTAL THERAPEUTICS

https://doi.org/10.1124/jpet.117.239905
J Pharmacol Exp Ther 361:441–453, June 2017

Detailed Characterization of the In Vitro Pharmacological and Pharmacokinetic Properties of *N*-(2-Hydroxybenzyl)-2, 5-Dimethoxy-4-Cyanophenylethylamine (25CN-NBOH), a Highly Selective and Brain-Penetrant 5-HT_{2A} Receptor Agonist[S]

Anders A. Jensen, John D. McCorvy, Sebastian Leth-Petersen, Christoffer Bundgaard, Gudrun Liebscher, Terry P. Kenakin, Hans Bräuner-Osborne, Jan Kehler, and Jesper Langgaard Kristensen

Department of Drug Design and Pharmacology, Faculty of Health and Medical Sciences, University of Copenhagen, Copenhagen, Denmark (A.A.J., S.L-P., G.L., H.B.-O., J.L.K.); Department of Pharmacology, University of North Carolina School of Medicine, Chapel Hill, North Carolina (J.D.M., T.P.K.); and Department of Discovery Chemistry and DMPK, H. Lundbeck A/S, Valby, Denmark (C.B., J.K.)

Received January 5, 2017; accepted February 23, 2017

ABSTRACT

Therapeutic interest in augmentation of 5-hydroxytryptamine$_{2A}$ (5-HT_{2A}) receptor signaling has been renewed by the effectiveness of psychedelic drugs in the treatment of various psychiatric conditions. In this study, we have further characterized the pharmacological properties of the recently developed 5-HT_2 receptor agonist *N*-2-hydroxybenzyl)-2,5-dimethoxy-4-cyanophenylethylamine (25CN-NBOH) and three structural analogs at recombinant 5-HT_{2A}, 5-HT_{2B}, and 5-HT_{2C} receptors and investigated the pharmacokinetic properties of the compound. 25CN-NBOH displayed robust 5-HT_{2A} selectivity in [^{3}H]ketanserin/[^{3}H]mesulergine, [^{3}H]lysergic acid diethylamide and [^{3}H]Cimbi-36 binding assays (K_i^{2C}/K_i^{2A} ratio range of 52–81; K_i^{2B}/K_i^{2A} ratio of 37). Moreover, in inositol phosphate and intracellular Ca^{2+} mobilization assays 25CN-NBOH exhibited 30- to 180-fold 5-HT_{2A}/5-HT_{2C} selectivities and 54-fold 5-HT_{2A}/5-HT_{2B} selectivity as measured by $\Delta\log(R_{max}/EC_{50})$ values. In an off-target screening 25CN-NBOH (10 μM) displayed either substantially weaker activity or inactivity at a plethora of other receptors, transporters, and kinases. In a toxicological screening, 25CN-NBOH (100 μM) displayed a benign acute cellular toxicological profile. 25CN-NBOH displayed high in vitro permeability ($P_{app} = 29 \times 10^{-6}$ cm/s) and low P-glycoprotein-mediated efflux in a conventional model of cellular transport barriers. In vivo, administration of 25CN-NBOH (3 mg/kg, s.c.) in C57BL/6 mice mice produced plasma and brain concentrations of the free (unbound) compound of ~200 nM within 15 minutes, further supporting that 25CN-NBOH rapidly penetrates the blood-brain barrier and is not subjected to significant efflux. In conclusion, 25CN-NBOH appears to be a superior selective and brain-penetrant 5-HT_{2A} receptor agonist compared with (±)-2,5-dimethoxy-4-iodoamphetamine (DOI), and thus we propose that the compound could be a valuable tool for future investigations of physiologic functions mediated by this receptor.

Introduction

The neurotransmitter serotonin [5-hydroxytryptamine (5-HT)] is widely distributed and regulates a broad spectrum of functions throughout the central nervous system (CNS) and in the peripheral nervous system (Berger et al., 2009). 5-HT mediates these effects through six classes of G protein-coupled receptors (GPCRs), 5-HT_1, 5-HT_2, 5-HT_4, 5-HT_5, 5-HT_6, and 5-HT_7, comprising a total of 13 receptor subtypes and a class of ligand-gated cation channels (5-HT_3) (Hannon and Hoyer, 2008; Millan et al., 2008; McCorvy and Roth, 2015). The 5-HT_{2A} receptor (5-HT_{2A}R), 5-HT_{2B} receptor (5-HT_{2B}R), and 5-HT_{2C} receptor (5-HT_{2C}R) are Gα_q-coupled receptors linked to activation of phospholipase C, increased formation of the second messengers inositol triphosphate and diacylglycerol, and mobilization of Ca^{2+} from intracellular stores, albeit the receptors also signal through other signaling cascades (Roth, 2011; Halberstadt, 2015; McCorvy and Roth, 2015; Maroteaux et al., 2017).

5-HT_{2A}R is the major postsynaptic 5-HT receptor in the CNS, where it is involved in processes of key importance for

This work was supported by the Novo Nordisk Foundation and the A.P. Møller Foundation for the Advancement of Medical Sciences.
https://doi.org/10.1124/jpet.117.239905.
[S] This article has supplemental material available at jpet.aspetjournals.org.

ABBREVIATIONS: 25CN-NBF, *N*-(2-fluorobenzyl)-2,5-dimethoxy-4-cyanophenylethylamine; 25CN-NBMD, *N*-(2,3-methylenedioxybenzyl)-2,5-dimethoxy-4-cyanophenylethylamine; 25CN-NBOH, *N*-(2-hydroxybenzyl)-2,5-dimethoxy-4-cyanophenylethylamine; 25CN-NBOMe, *N*-(2-methoxybenzyl)-2,5-dimethoxy-4-cyanophenylethylamine; 5-HT, 5-hydroxytryptamine (serotonin); 5-HT_{2A}R, 5-hydroxytryptamine type 2A receptor; 5-HT_{2B}R, 5-hydroxytryptamine type 2B receptor; 5-HT_{2C}R, 5-hydroxytryptamine type 2C receptor; 5-HT_2R, 5-hydroxytryptamine type 2 receptor; CNS, central nervous system; DOI, (±)-2,5-dimethoxy-4-iodoamphetamine; GPCR, G protein-coupled receptor; HBSS, Hanks' buffered saline solution; IP, inositol phosphate; IP_1, inositol monophosphate; LSD, lysergic acid diethylamide; MDCK, Madin-Darby canine kidney.

memory and cognitive functions, mood, circadian rhythm, and appetite (Berger et al., 2009; Zhang and Stackman, 2015). The receptor constitutes a major drug target in cognitive and psychiatric disorders (Celada et al., 2004; González-Maeso and Sealfon, 2009; Meltzer, 2012; Maroteaux et al., 2017), and it is the main mediator of the psychotropic and psychotomimetic effects of natural hallucinogens such as lysergic acid diethylamide (LSD), psilocybin, and mescaline as well as several synthetic drugs (González-Maeso and Sealfon, 2009; Halberstadt, 2015; Nichols, 2016; Nichols et al., 2017). For decades, the hallucinogenic properties possessed by these drugs has hampered the exploration of the therapeutic potential in augmentation of 5-HT_{2A}R signaling for treatment of CNS disorders. However, in recent years the remarkable effects mediated by LSD and psilocybin in rodent models of cognitive and psychiatric disorders and in human treatment trials of depression, posttraumatic stress, obsessive-compulsive disorder, autism, and various forms of addiction have substantiated this potential and rekindled the therapeutic interest in 5-HT_{2A}R agonists (Kometer et al., 2012; Halberstadt, 2015; Schmid et al., 2015; Carhart-Harris et al., 2016; Nichols, 2016; Maroteaux et al., 2017; Nichols et al., 2017).

Classical 5-HT_{2A}R agonists can be divided into three structural classes: ergolines, tryptamines, and phenethylamines, represented by LSD, psilocybin, and mescaline, respectively. The hallucinogenic effects induced by these drugs are believed to arise predominantly from their 5-HT_{2A}R activity; however, the compounds also exhibit potent activities at other 5-HT receptors and in some cases at other monoaminergic receptors as well (Nichols, 2016). The polypharmacological profiles of these drugs complicate their use as pharmacological tools for studies of physiologic 5-HT_{2A}R functions. Thus far, the prototypic 5-HT type 2 receptor (5-HT_2R) agonist (±)-2,5-dimethoxy-4-iodoamphetamine (DOI) has been used extensively to probe 5-HT_{2A}R functions in vivo; however, since DOI only displays modest preference for 5-HT_{2A}R over 5-HT_{2B}R and 5-HT_{2C}R (Almaula et al., 1996; Nelson et al., 1999; Pigott et al., 2012; Canal et al., 2013) it has often been applied in combination with 5-HT_2R subtype-selective antagonists in previous studies. Because of its inherent selectivity for 5-HT_2Rs over other serotonergic and monoaminergic receptors, the phenethylamine scaffold has often been applied as a lead in the search for selective 5-HT_{2A}R agonists (Rickli et al., 2015; Nichols, 2016), but the fact that the orthosteric sites in the three 5-HT_2R subtypes are highly conserved has made the development of truly 5-HT_{2A}R-selective agonists difficult. However, a couple of *N*-benzylphenethylamine derivatives have recently been reported to exhibit substantial degrees of 5-HT_{2A}R-over-5-HT_{2C}R selectivity (Juncosa et al., 2013; Hansen et al., 2014, 2015). One of these analogs, *N*-(2-hydroxybenzyl)-2,5-dimethoxy-4-cyanophenylethylamine [(25CN-NBOH), compound 1] (Fig. 1), was originally reported to display 100- and 90-fold selectivity for 5-HT_{2A}R over 5-HT_{2C}R in radioligand binding and inositol phosphate (IP) turnover assays, respectively (Hansen et al., 2014). Subsequently, 25CN-NBOH has been used as a pharmacological tool in studies of 5-HT_{2A}R functions in connection with time perception and hallucinogen-induced head twitches in mice (Fantegrossi et al., 2015; Halberstadt et al., 2016) and to elucidate the involvement of the receptor in mitochondrial biogenesis (Harmon et al., 2016).

In the present study, we have characterized the in vitro pharmacological and pharmacokinetic properties of 25CN-NBOH in detail. 25CN-NBOH and three close structurally related analogs {*N*-(2-methoxybenzyl)-2,5-dimethoxy-4-cyanophenylethylamine [(25CN-NBOMe), compound 2], *N*-(2-fluorobenzyl)-2,5-dimethoxy-4-cyanophenylethylamine [(25CN-NBF), compound 3], and *N*-(2,3-methylenedioxybenzyl)-2,5-dimethoxy-4-cyanophenylethylamine [(25CN-NBMD), compound 4]} (Fig. 1) have been subjected to elaborate pharmacological characterization and compared with DOI at recombinant 5-HT_2Rs in binding and functional assays. Moreover, 25CN-NBOH has been screened for off-target activity at other monoamine receptors and several other putative targets. Finally, the pharmacokinetic characteristics of 25CN-NBOH have been investigated, including the brain and plasma exposure of the drug following administration in mice.

Materials and Methods

Materials. Culture media, serum, antibiotics, and buffers for cell culture were obtained from Invitrogen (Paisley, United Kingdom). The Fluo-4/AM dye was obtained from Molecular Probes (Eugene, OR), and the IP-One assay kit was purchased from Cisbio (Bagnols, France). 5-HT and probenecid were purchased from Sigma-Aldrich (St. Louis, MO), and the Polyfect transfection reagent was obtained from Qiagen (Hilden, Germany). Compounds 1–4 and DOI were synthesized in-house as previously described (Hansen et al., 2014), and [^{3}H]Cimbi-36 was kindly provided by Dr. Christer Halldin (Karolinska Institute, Stockholm, Sweden).

Cell Culture and Transfections. All cell lines were cultured in a humidified atmosphere at 37°C and 5% CO_2. Tetracycline-inducible Flp-In293 cells (Invitrogen) stably expressing either human 5-HT_{2A}R, 5-HT_{2B}R, or 5-HT_{2C}R-INI (Cheng et al., 2016) were used for Ca^{2+} assay I and cultured in Dulbecco's modified Eagle's medium

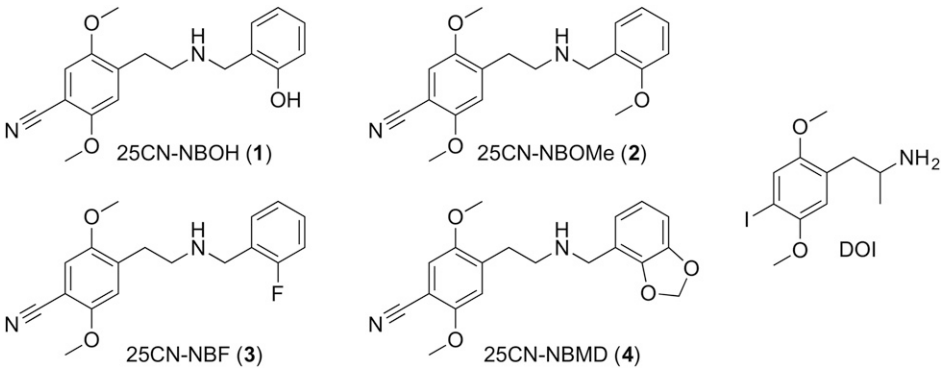

Fig. 1. Chemical structures of the four analogs and DOI.

supplemented with penicillin (100 U/ml), streptomycin (100 μg/ml), and 5% fetal bovine serum containing 100 μg/ml hygromycin B (KSE Scientific, Durham, North Carolina) and 10 μg/ml blasticydin (Invivogen) as selection antibiotics. The HEK293 cell lines stably expressing human 5-HT_{2A}R and 5-HT_{2C}R (Jensen et al., 2013) used for the IP-One assay and Ca^{2+} assay II were cultured in Dulbecco's modified Eagle's medium supplemented with penicillin (100 U/ml), streptomycin (100 μg/ml), and 5% dialyzed fetal bovine serum supplemented with 1 mg/ml G-418. The tsA201 cells used for the [^{3}H]Cimbi-36 binding experiments were cultured in Dulbecco's modified Eagle's medium supplemented with penicillin (100 U/ml), streptomycin (100 μg/ml), and 10% fetal bovine serum. For the transfections of tsA201 cells, 1.8×10^6 cells were split into a 10-cm tissue culture plate and transfected the following day with a total of 8 μg cDNA (5-HT_{2A}-pcDNA3.1 or 5-HT_{2C}-pcDNA3.1) plasmids using Polyfect according to the manufacturer's procedure (Qiagen).

[^{3}H]Ketanserin, [^{3}H]Mesulergine, and [^{3}H]LSD Binding Assays. Membranes were prepared from tetracycline-inducible Flp-In293 stably expressing either human 5-HT_{2A}R, 5-HT_{2B}R, or 5-HT_{2C}R-INI, and radioligand binding assays were performed as previously described (Cheng et al., 2016). Briefly, membranes were resuspended in standard binding buffer (50 mM Tris, 10 mM $MgCl_2$, 0.1 mM EDTA, 0.1% bovine serum albumin, 0.01% ascorbic acid, pH 7.4) and added to 96-well polypropylene plates containing test ligands (1 pM to 100 μM, final concentrations). For 5-HT_{2A}R affinity determination, either [^{3}H]LSD (K_D = 0.17 nM, concentration range 0.3–0.8 nM) or [^{3}H]ketanserin (K_D = 1.5 nM, concentration range 0.9–1.7 nM) was used. For 5-HT_{2B}R affinity determination, [^{3}H]LSD (K_D = 0.36 nM, concentration range 0.6–1.2 nM) was used. For 5-HT_{2C}R affinity determination, either [^{3}H]LSD (K_D = 4.3 nM, concentration range 1.5–3.0 nM) or [^{3}H]mesulergine (K_D = 2.3 nM, concentration range 2.5–3.3 nM) was used. Reactions were incubated at 37°C for 2 hours in the dark to reach equilibrium and terminated by harvesting onto 0.3% polyethyleneimine–soaked Filtermax GF/A filters (PerkinElmer, Waltham, MA). Filters were washed three times with ice-cold harvest buffer (50 mM Tris, pH 7.4), dried, and Melitilex scintillant (PerkinElmer, Waltham, MA) was applied. Filters were counted on a Wallac TriLux microbeta counter (1 minute/well). Bound radioligand was plotted as a function of log[ligand] and data were analyzed using a one-site K_i model built into the Graphpad Prism 5.0 software (Graphpad, La Jolla, CA).

[^{3}H]Cimbi-36 Binding Assay. The binding affinities of the ligands at human 5-HT_{2A}R and 5-HT_{2C}R using [^{3}H]Cimbi-36 as the radioligand were determined at membranes from tsA201 cells transiently expressing the two receptors. Next, 36–48 hours after the transfection, the tsA201 cells were harvested and scraped into ice-cold assay buffer (50 mM Tris–HCl, 4 mM $CaCl_2$, pH 7.4), homogenized with a Polytron homogenizer (Kinematica, Eschbach, Germany) for 10 seconds, and centrifuged for 20 minutes at 50,000*g* at 4°C. Cell pellets were resuspended in fresh assay buffer, homogenized, and centrifuged at 50,000*g* for another 20 minutes, after which the membranes were stored at −80°C until use. On the day of the assay, the cell membranes were resuspended in assay buffer and incubated with [^{3}H]Cimbi-36 and various concentrations of the test compounds. Concentration ranges of 0.05–0.15 and 0.2–0.5 nM [^{3}H]Cimbi-36 were used for the affinity determinations at 5-HT_{2A}R (K_D = 0.11 nM) and 5-HT_{2C}R (K_D = 1.5 nM), respectively. Nonspecific binding was determined using 20 μM mianserin, and the assay volume was 1 ml. The reactions were incubated for 2 hours at room temperature while shaking. Whatman GF/C filter (GE Healthcare, Brøndby, Denmark) were presoaked for 1 hour in a 0.2% polyethylenimine solution, and binding was terminated by filtration through the filters using a 48-well Brandel cell harvester (Alpha Biotech Ltd, Glasgow, United Kingdom) and four washes with 4 ml of ice-cold isotonic NaCl solution. After this, the filters were dried, 3 ml of Opti-Fluor (PerkinElmer) was added, and the amount of bound radioactivity was determined in a scintillation counter.

IP One HTRF Assay. The ligands were characterized functionally at the stable 5-HT_{2A}R- and 5-HT_{2C}R-HEK293 cell lines in the IP One HTRF Assay (IP-One homogeneous time-resolved fluorescence assay) (Nørskov-Lauritsen et al., 2014) essentially as previously described (Jensen et al., 2013; Hansen et al., 2015). On the day of the experiment subconfluent cells were washed one time with phosphate-buffered saline and detached from the cell culture plate using dissociation buffer (Sigma-Aldrich). Cells were centrifuged and resuspended in assay buffer [Hanks' buffered saline solution (HBSS) supplemented with 20 mM HEPES, 1 mM $CaCl_2$, and 1 mM $MgCl_2$, pH 7.4] at a concentration of 1×10^7 cells/ml. Ligand solutions were prepared in HBSS supplemented with 1 mM $CaCl_2$, 1 mM $MgCl_2$, and 40 mM LiCl. Then, 5 μl of ligand solution was mixed with 5 μl cell suspension in a white 384-well OptiPlate (PerkinElmer). The plate was sealed and incubated at 37°C for 1 hour, followed by 15-minute incubation at room temperature. Next, 10 μl of detection reagents [lysis buffer containing 2.5% Tb^{3+}-anti-inositol monophosphate (IP_1) antibody and 2.5% IP_1-d2] was added and the plate was incubated for 1 hour at room temperature. The plate was read on an Envision plate reader (PerkinElmer) exciting the cells with light at 340 nm and measuring emitted light at 620 and 665 nm. In this assay, the time resolved-fluorescence resonance energy transfer 665/620 nm ratio was inversely proportional to the IP_1 accumulation in the cells upon 5-HT_{2A}R or 5-HT_{2C}R activation. The Förster resonance energy transfer ratios were converted to IP_1 concentrations by interpolating values from an IP_1 standard curve generated from a calibrator provided by the manufacturer (Cisbio, Codolet, France). The compounds were characterized in triplicate at least three times at each cell line.

Ca^{2+} Assay I. This calcium flux assay used tetracycline-inducible Flp-In293 stably expressing either human 5-HT_{2A}R, 5-HT_{2B}R, or 5-HT_{2C}R-INI and a $FLIPR^{TETRA}$ fluorescence imaging plate reader (Molecular Dynamics Sunnyvale, CA), which has been previously described (Cheng et al., 2016). Briefly, cells were seeded (10,000 cells per well in 40 μl volume) into poly-L-lysine-coated 384-well black plates followed by addition of 2 μg/ml tetracycline to induce receptor expression. On the day of the assay, the medium was decanted and replaced with drug buffer (20 μl/well, 1X HBSS, 20 mM HEPES, 0.1% bovine serum albumin, 0.01% ascorbic acid, pH 7.4) containing Fluo-4 Direct Dye (Invitrogen). Plates containing dye were incubated for 1 hour at 37°C. Afterward, cells were challenged with 10 μl/well of drug (concentration range 1 pM to 32 μM) at 3X final concentration diluted in drug buffer. Calcium flux was measured (1 read/s) for 300 seconds. Fluorescence in each well was normalized to the average of the first 10 reads, and maximum-fold increase was determined. Fold over baseline was plotted as a function of drug concentration. Data were normalized to the percentage of 5-HT stimulation and analyzed using log[agonist] versus response in Graphpad Prism 5.0.

Ca^{2+} Assay II. The test and reference ligands were characterized functionally at the stable 5-HT_{2A}R- and 5-HT_{2C}R-HEK293 cell lines in this assay essentially as previously described (Jensen et al., 2013). Briefly, the cells were split into poly-D-lysine-coated black 96-well plates with clear bottoms (6×10^4 cells/well). The following day the culture medium was aspirated and the cells were incubated in 50 μl assay buffer [HBSS containing 20 mM HEPES, 1 mM $CaCl_2$, 1 mM $MgCl_2$, 2.5 mM probenecid, pH 7.4] supplemented with 6 mM Fluo-4/AM at 37°C for 1 hour. Next, the buffer was aspirated, the cells were washed once with 100 μl assay buffer, and then 100 μl assay buffer was added to the cells (in the antagonist experiments the antagonist was added at this point). The 96-well plate was assayed in FLEXStation^3 (Molecular Devices, Crawley, United Kingdom) measuring emission (in fluorescence units) at 525 nm caused by excitation at 485 nm before and up to 90 seconds after addition of 33.3 μl test compound solution in the assay buffer. The compounds were characterized in duplicate at least three times at each cell line.

Data Analysis—Calculation of $\Delta\log(R_{max}/EC_{50})$ Values. The Black/Leff operational model (Black and Leff, 1983) can be used to compare the relative potencies of full to partial agonists through the parameter $\Delta\log(\tau/K_A)$, which specifically is the difference in the logarithms of the ratio of the efficacy (τ) and the equilibrium-dissociation constant (K_A) of the two relevant agonists. A further simplification of this parameter can be made if the slopes of

the agonist concentration-response curves are not significantly different from unity. As shown by Black et al. (1985), the maximal response to an agonist is given by

$$R_{max} = \frac{\tau^n E_{max}}{1 + \tau^n} \quad (1)$$

Similarly, the EC_{50} value for an agonist is given by

$$EC_{50} = \frac{K_A}{\left[(2 + \tau^n)^{1/n} - 1\right]} \quad (2)$$

It can be seen that for $n = 1$, eqs. 1 and 2 yield a ratio of $R_{max}/EC_{50} = \tau/K_A$. Therefore, the $\Delta\log(R_{max}/EC_{50})$ values furnish system-independent values to compare the relative activity of agonists (Kenakin, 2017).

In Vitro Screening of 25CN-NBOH at Various Targets. The selectivity profile of 25CN-NBOH (compound 1) was investigated in radioligand binding assays at numerous targets performed by the National Institute of Mental Health's Psychoactive Drug Screening Program (http://pdsp.med.unc.edu/pdspw/binding.php) (Besnard et al., 2012) and by Eurofins Cerep SA, (Cell L'Evescault, France). In these binding assays, an assay concentration of 10 μM 25CN-NBOH was tested at homogenates of mammalian cell lines expressing different targets, with a few assays being performed using homogenized rat brain tissue, using an assay concentration of the radioligand near or at the K_D value for the specific target. 25CN-NBOH was also tested by Eurofins at a broad range of kinases and other enzymes in enzymatic assays. The hERG channel inhibition was determined to evaluate the potential of 25CN-NBOH to induce cardiac arrhythmia.

Toxicology Screening. The cellular toxicity was investigated in a high-content screening assay, where the effects of 25CN-NBOH at concentrations up to 100 μM for six parameters (nuclei counts, nuclear area, plasma membrane integrity, lysosomal activity, mitochondrial membrane potential, and mitochondrial area) were determined (Persson et al., 2013).

Solubility. The solubility and stability of 25CN-NBOH at pH 7.4 was determined.

Membrane Permeability, Intrinsic Clearance, and Plasma Protein and Brain Tissue Binding. The bidirectional permeability of 25CN-NBOH was measured in the Madin-Darby canine kidney (MDCK) cell line expressing human MDR1 (P-glycoprotein) in triplicate as described previously (Risgaard et al., 2013). The permeability assessment was performed at 37°C over a 60-minute period at a concentration of 0.5 μM applied to the apical or basolateral side of the cell monolayer. The efflux ratio was calculated as the ratio between the permeability in the basal-to-apical direction divided by the permeability in the apical-to-basal direction. The murine intrinsic clearance of 25CN-NBOH (in l/kg/h) was calculated from its half-life in the presence of murine microsomes, as previously described (Leth-Petersen et al., 2014). The free fraction of 25CN-NBOH in mouse plasma and brain tissue was determined in vitro at 37°C in triplicate using equilibrium dialysis as described previously (Redrobe et al., 2014). The assay was performed using a test compound concentration of 1 μM incubated for 5 hours.

Plasma and Brain Exposure Analysis. Three groups of male C57BL/6 mice (20–25 g, obtained from Charles River, Sulzfeld, Germany) were dosed subcutaneously with 3 mg/kg of 25CN-NBOH. The compound was dissolved in 20% hydroxypropyl-β-cyclodextrin dosed in a volume of 10 ml/kg. Plasma and brain samples were taken from each group at 5, 15, or 30 minutes after drug administration (n = 3). Under isoflurane anesthesia, cardiac blood was obtained in EDTA-coated tubes and centrifuged for 10 minutes at 4°C, after which plasma was harvested. After decapitation, the brain was removed and gently rinsed on filter paper and frozen together with plasma specimens at −80°C until analysis. Brain homogenate was prepared by homogenizing the brain with four volumes of deionized water using isothermal focused acoustic ultrasonication (Covaris Inc., Woburn, MA). Quantitative bioanalysis was performed using ultraperformance liquid chromatography (Waters, Milford, MA) coupled to tandem mass spectrometry (Sciex 4000; AB Sciex, Foster City, CA). The lower limit of quantification was 1 ng/ml in plasma and 5 ng/g in brain tissue. Ethical permission for the in vivo procedures was granted by the Danish Animal Experiments Inspectorate (Glostrup, Denmark), and all animal procedures were performed in compliance with Directive 2010/63/EU of the European Parliament and the Council and with Danish Law and Order regulating animal experiments.

Results

Binding Properties of the Four Analogs and DOI at Human 5-HT_{2A}R and 5-HT_{2C}R

The binding affinities of 25CN-NBOH (compound 1), 25CN-NBOMe (compound 2), 25CN-NBF (compound 3), 25CN-NBMD (compound 4), and DOI to recombinant human 5-HT_{2A}R, 5-HT_{2B}R, and 5-HT_{2C}R were determined in competition binding experiments using membranes from mammalian cell lines expressing the three receptors. Since previous studies have found binding affinities exhibited by agonists at 5-HT_{2A}R and other GPCRs to be highly dependent on the intrinsic activity of the radioligand used (Rosenkilde et al., 1994; Hjorth et al., 1996; Sleight et al., 1996; Sagan et al., 1997; Rosenkilde and Schwartz, 2000), the binding affinities of the compounds were determined using both antagonist ([^{3}H]ketanserin for 5-HT_{2A}R and [^{3}H]mesulergine for 5-HT_{2C}R) and agonist (the partial agonist [^{3}H]LSD for 5-HT_{2A}R, 5-HT_{2B}R, and 5-HT_{2C}R and the partial/full agonist [^{3}H]Cimbi-36 for 5-HT_{2A}R and 5-HT_{2C}R) radioligands. The fact that the binding experiments were performed using different protocols, and in the case of 5-HT_{2A}R and 5-HT_{2C}R using cell lines with different receptor expression levels, provided detailed and unbiased insight into the binding characteristics of the compounds.

The respective binding affinities displayed by the five compounds at 5-HT_{2A}R and 5-HT_{2C}R in different binding assays were largely comparable (Fig. 2; Tables 1 and 2). For example, the K_i values for 25CN-NBOH at 5-HT_{2A}R using [^{3}H]ketanserin, [^{3}H]LSD, and [^{3}H]Cimbi-36 assays were 1.1, 0.81, and 1.7 nM, respectively, and the K_i values at 5-HT_{2C}R using [^{3}H]mesulergine, [^{3}H]LSD, and [^{3}H]Cimbi-36 assays were 89, 42, and 130 nM, respectively. Consequently, the rank orders of the binding affinities of the five compounds in the binding assays were also comparable: DOI ~ 25CN-NBOH ~ 25CN-NBOMe > 25CN-NBMD > 25CN-NBF. 25CN-NBOH and 25CN-NBMD displayed K_i^{2B}/K_i^{2A} ratios of 37 and 33 in in the [^{3}H]LSD assay and K_i^{2C}/K_i^{2A} ratio ranges of 52–81 and 65–263 in the [^{3}H]ketanserin/[^{3}H]mesulergine, [^{3}H]LSD, and [^{3}H]Cimbi-36 assays, respectively, and thus they were the most 5-HT_{2A}R-selective ligands of the four analogs. In comparison, DOI displayed a 2.6-fold higher binding affinity at 5-HT_{2A}R than at 5-HT_{2B}R in the [^{3}H]LSD assay and 3.6- to 19-fold higher binding affinities at 5-HT_{2A}R than 5-HT_{2C}R in the [^{3}H]ketanserin/[^{3}H]mesulergine, [^{3}H]LSD, and [^{3}H]Cimbi-36 assays (Fig. 2; Tables 1 and 2).

Functional Properties of the Four Analogs and DOI at Human 5-HT_{2A}R, 5-HT_{2B}R and 5-HT_{2C}R

In our previous study, the functional properties of DOI and the four analogs were characterized at human 5-HT_{2A}R and 5-HT_{2C}R transiently expressed in tsA201 cells in a conventional IP turnover assay measuring accumulation of [^{3}H]IP_{1-3}

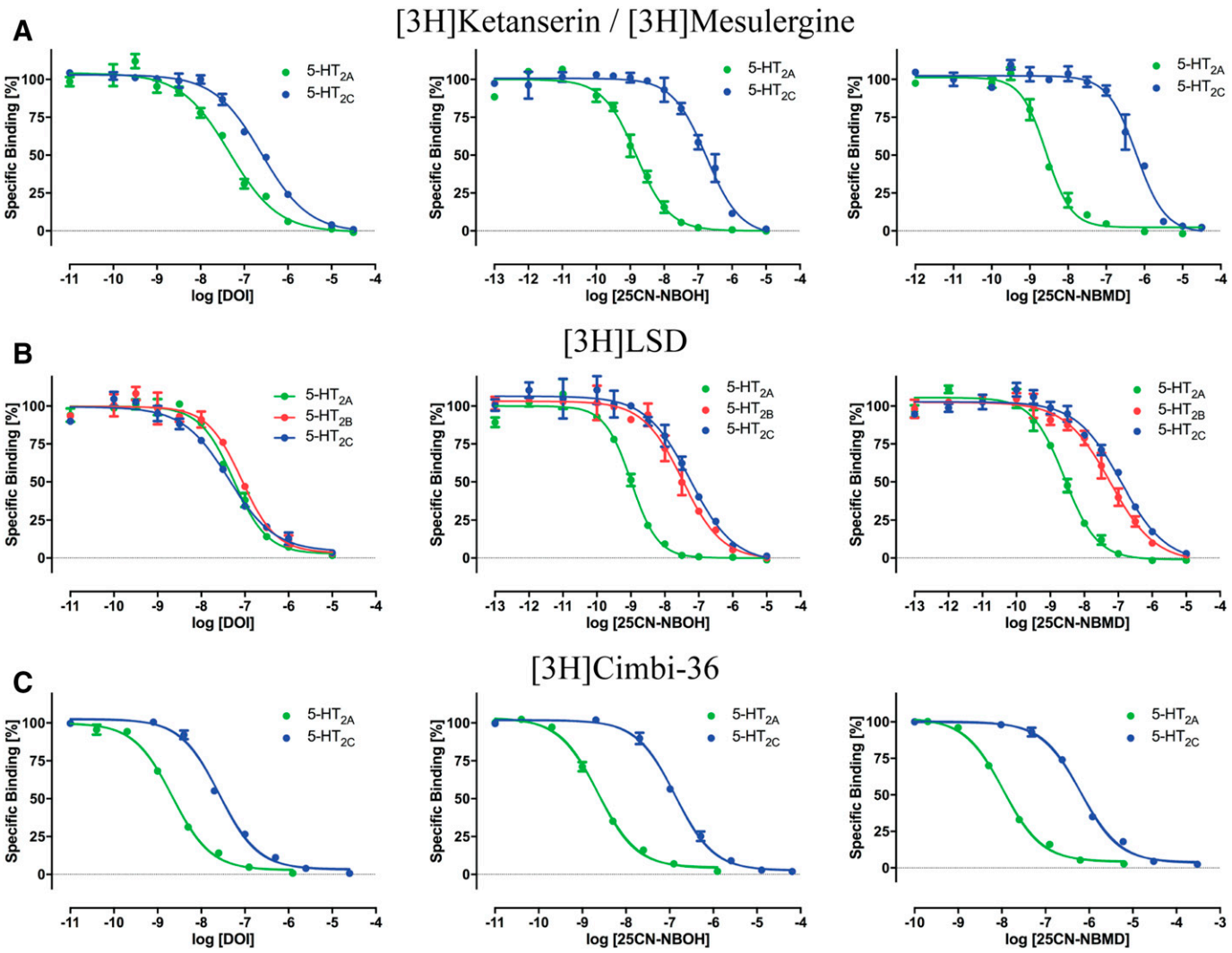

Fig. 2. Binding properties displayed by DOI, 25CN-NBOH, and 25CN-NBMD at human 5-HT$_2$ receptors in radioligand competition binding assays. (A) Concentration-inhibition curves for DOI, 25CN-NBOH, and 25CN-NBMD at 5-HT$_{2A}$R and 5-HT$_{2C}$R in [^{3}H]ketanserin and [^{3}H]mesulergine binding assays, respectively. Tracer concentrations of 1.3 nM [^{3}H]ketanserin and 3.3 nM [^{3}H]mesulergine were used in the 5-HT$_{2A}$R and 5-HT$_{2C}$R binding experiments, respectively. (B) Concentration-inhibition curves for DOI, 25CN-NBOH, and 25CN-NBMD at 5-HT$_{2A}$R, 5-HT$_{2B}$R, and 5-HT$_{2C}$R in the [^{3}H]LSD binding assay. [^{3}H]LSD concentrations of 0.8, 1.2, and 3.0 nM were used in the 5-HT$_{2A}$R, 5-HT$_{2B}$R, and 5-HT$_{2C}$R binding experiments, respectively. (C) Concentration-inhibition curves for DOI, 25CN-NBOH, and 25CN-NBMD at 5-HT$_{2A}$R and 5-HT$_{2C}$R in the [^{3}H]Cimbi-36 binding assay. [^{3}H]Cimbi-36 concentrations of 0.1 and 0.2 nM were used in the 5-HT$_{2A}$R and 5-HT$_{2C}$R binding experiments, respectively.

(Hansen et al., 2014). In the present study, functional properties of the compounds were determined at the two receptors stably expressed in HEK293 cells in the Förster resonance energy transfer–based IP One HTRF assay. In this assay, the formation and accumulation of IP$_1$ upon activation of the receptors was measured based on homogenous time-resolved Förster resonance energy transfer between terbium cryptate–labeled anti-IP$_1$ antibody and d2-labeled IP$_1$ (Nørskov-Lauritsen et al., 2014),

TABLE 1

Binding affinities displayed by DOI, 25CN-NBOH, 25CN-NBOMe, 25CN-NBF, and 25CN-NBMD at human 5-HT$_{2A}$R and 5-HT$_{2C}$R in competition binding assays using the antagonists [^{3}H]ketanserin and [^{3}H]mesulergine as radioligands

The binding assays were performed as described in *Materials and Methods*. The K_i values are given in nM with the pK_i ± S.E.M. values in brackets and the number of experiments (n) for each binding affinity given in superscript.

	K_i [pK_i ± S.E.M.]	
	5-HT$_{2A}$R ([^{3}H]ketanserin)	5-HT$_{2C}$R ([^{3}H]mesulergine)
DOI	27 [7.57 ± 0.01] $^{(3)}$	110 [6.98 ± 0.05] $^{(3)}$
25CN-NBOH (compound 1)	1.1 [8.96 ± 0.03] $^{(3)}$	89 [7.05 ± 0.01] $^{(3)}$
25CN-NBOMe (compound 2)	3.9 [8.42 ± 0.09] $^{(3)}$	180 [6.74 ± 0.02] $^{(3)}$
25CN-NBF (compound 3)	96 [7.02 ± 0.04] $^{(3)}$	2500 [5.61 ± 0.03] $^{(3)}$
25CN-NBMD (compound 4)	1.9 [8.73 ± 0.03] $^{(3)}$	500 [6.30 ± 0.03] $^{(3)}$

TABLE 2

Binding affinities displayed by DOI, 25CN-NBOH, 25CN-NBOMe, 25CN-NBF, and 25CN-NBMD at human 5-HT_{2A}R, 5-HT_{2B}R, and 5- HT_{2C}R in competition binding assays using the partial agonist [^{3}H]LSD and the partial/full agonist [^{3}H]Cimbi-36 as radioligands

The binding assays were performed as described in *Materials and Methods*. The K_i values are given in nM with the pK_i ± S.E.M. values in brackets and the number of experiments (n) for each binding affinity given in superscript.

	K_i [pK_i ± S.E.M.]				
	[^{3}H]LSD			[^{3}H]Cimbi-36	
	5-HT_{2A}R	5-HT_{2B}R	5-HT_{2C}R	5-HT_{2A}R	5-HT_{2C}R
DOI	8.1 [8.11 ± 0.10] $^{(3)}$	21 [7.72 ± 0.13] $^{(3)}$	29 [7.55 ± 0.02] $^{(3)}$	1.3 [8.88 ± 0.11] $^{(3)}$	25 [7.61 ± 0.10] $^{(3)}$
25CN-NBOH (compound 1)	0.81 [9.09 ± 0.02] $^{(3)}$	30 [7.52 ± 0.00] $^{(3)}$	42 [7.39 ± 0.11] $^{(3)}$	1.7 [8.77 ± 0.09] $^{(4)}$	130 [6.89 ± 0.06] $^{(3)}$
25CN-NBOMe (compound 2)	1.8 [8.78 ± 0.11] $^{(3)}$	47 [7.34 ± 0.07] $^{(3)}$	40 [7.42 ± 0.10] $^{(3)}$	2.1 [8.67 ± 0.07] $^{(4)}$	8 [7.11 ± 0.07] $^{(3)}$
25CN-NBF (compound 3)	31 [7.51 ± 0.07] $^{(3)}$	380 [6.42 ± 0.02] $^{(3)}$	850 [6.07 ± 0.04] $^{(3)}$	130 [6.90 ± 0.13] $^{(4)}$	1,500 [5.81 ± 0.06] $^{(4)}$
25CN-NBMD (compound 4)	2.0 [8.70 ± 0.02] $^{(3)}$	65 [7.21 ± 0.14] $^{(3)}$	130 [6.88 ± 0.09] $^{(3)}$	6.9 [8.16 ± 0.04] $^{(4)}$	630 [6.20 ± 0.04] $^{(3)}$

and in a previous study 5-HT and the reference 5-HT_2R agonists PNU 22394, CP 809101, and MK-212 exhibited functional properties at the 5-HT_{2A}R- and 5-HT_{2C}R-HEK293 cell lines in this assay that were in good agreement with the literature (Jensen et al., 2013).

The rank orders of agonist potencies and the 5-HT_{2A}R/5-HT_{2C}R selectivity ratios exhibited by DOI and the four analogs in this assay were in excellent agreement with those observed for the agonists in the [^{3}H]IP_{1-3} assay (Fig. 3A; Table 3). In fact, even the absolute EC_{50} values displayed by the compounds at the receptors were strikingly similar between the two assays (Table 3). Analogous to their profiles in the [^{3}H]IP_{1-3} assay, 25CN-NBOH (compound 1) and 25CN-NBOMe (compound 2) were only slightly more potent 5-HT_{2A}R agonists (~2-fold) than DOI in the IP-One assay, and thus it was primarily the 7.6- and 5-fold higher EC_{50} values exhibited by compounds 1 and 2 compared with DOI at 5-HT_{2C}R that gave rise to their higher 5-HT_{2A}R/5-HT_{2C}R selectivity ratios (Fig. 3A; Table 3). 25CN-NBF (compound 3) and 25CN-NBMD (compound 4) were substantially weaker agonists at the two receptors, and thus the rank order of agonist potencies displayed by the compounds at 5-HT_{2A}R was the same as the order of their binding affinities at the receptor: DOI ~ 25CN-NBOH ~ 25CN-NBOMe > 25CN-NBMD > 25CN-NBF. However, 25CN-NBF and 25CN-NBMD displayed comparable potencies at 5-HT_{2C}R, and thus 25CN-NBMD exhibited roughly the same degree of selectivity for 5-HT_{2A}R over 5-HT_{2C}R as 25CN-NBOH (Fig. 3A; Table 3). DOI and the four analogs were all partial agonists at 5-HT_{2A}R, exhibiting maximal responses of 61%–87% of that elicited by 5-HT. DOI, 25CN-NBOH, and 25CN-NBOMe were full agonists at 5-HT_{2C}R, whereas 25CN-NBF and 25CN-NBMD were partial agonists. Thus, the intrinsic activities of the five

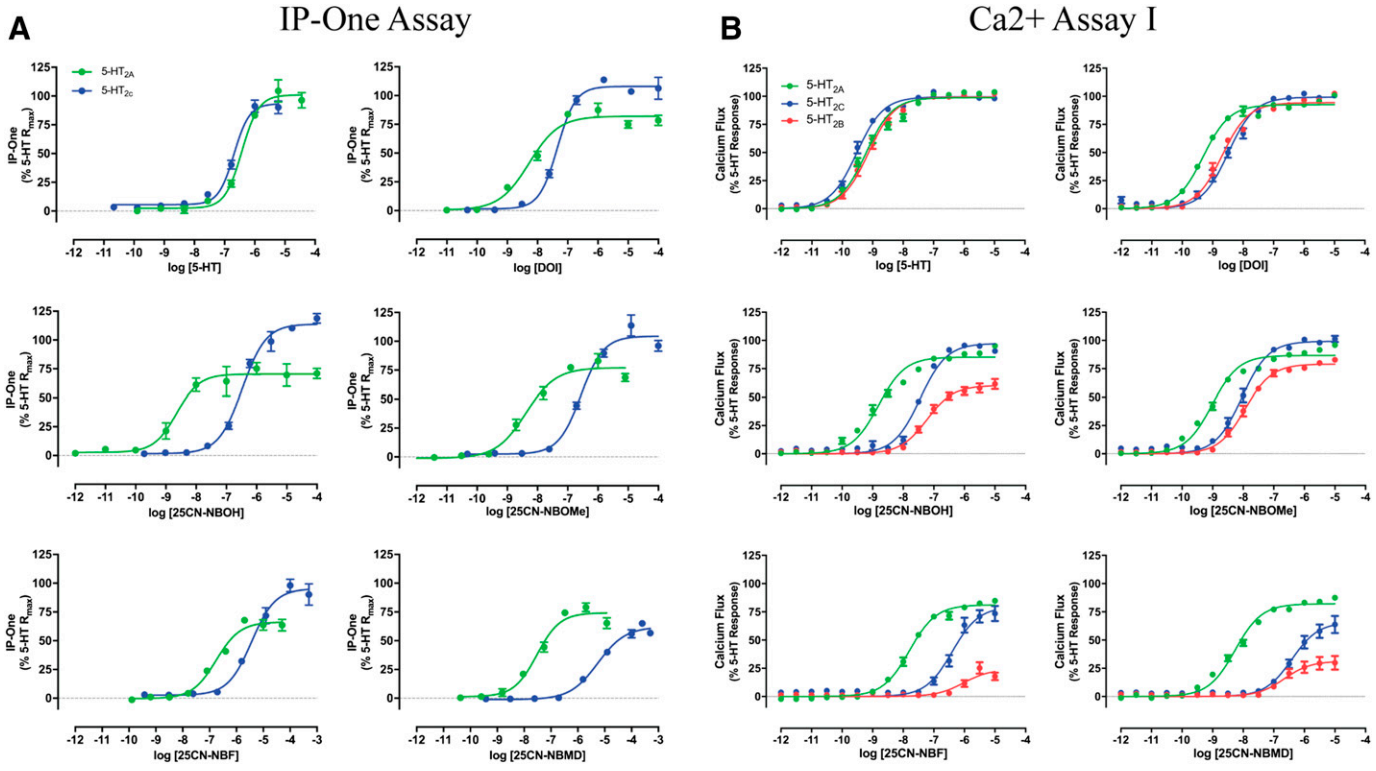

Fig. 3. Agonist properties displayed by 5-HT, DOI, 25CN-NBOH, 25CN-NBOMe, 25CN-NBF, and 25CN-NBMD at human 5-HT_2Rs in two functional assays. (A) Concentration-response curves of the six agonists at stable 5-HT_{2A}R- and 5-HT_{2C}R-HEK293 cell lines in the IP-One assay. (B) Concentration-response curves of the six agonists at 5-HT_{2A}R-, 5-HT_{2B}R-, and 5-HT_{2C}R-INI Flp-In293 cell lines in Ca^{2+} assay I.

TABLE 3

Agonist properties displayed by 5-HT, DOI and compounds 1–4 at human 5-HT$_{2A}$R and 5-HT$_{2C}$R expressed in mammalian cell lines in the [^{3}H]IP$_{1\text{-}3}$ and IP-One assays

The functional assays were performed as described in *Materials and Methods*. The EC_{50} values are given in nM with the pEC_{50} ± S.E.M. values in brackets and the R_{max} ± S.E.M. values given as the percentage of the maximal response induced by 5-HT. The number of experiments (n) for each set of potency and efficacy data are given in superscript.

	[^{3}H]IP$_{1\text{-}3}$ Assay[a]		IP-One Assay	
	5-HT$_{2A}$R	5-HT$_{2C}$R	5-HT$_{2A}$R	5-HT$_{2C}$R
	EC_{50} [EC_{50} ± S.E.M.] R_{max} ± S.E.M.	EC_{50} [EC_{50} ± S.E.M.] R_{max} ± S.E.M.	EC_{50} [EC_{50} ± S.E.M.] R_{max} ± S.E.M.	EC_{50} [EC_{50} ± S.E.M.] R_{max} ± S.E.M.
5-HT	9.5 [8.02 ± 0.04] 100	4.4 [8.36 ± 0.09] 100	300 [6.52 ± 0.06] 100 $^{(21)}$	190 [6.72 ± 0.07] 100 $^{(18)}$
DOI	2.9 [8.54 ± 0.02] 93 ± 5	28 [7.56 ± 0.07] 100 ± 2	6.3 [8.20 ± 0.03] 87 ± 3 $^{(4)}$	46 [7.34 ± 0.08] 119 ± 8 $^{(3)}$
25I-NBOMe	0.72 [9.14 ± 0.14] 90 ± 3	18 [7.74 ± 0.16] 96 ± 2	n.t.	n.t.
Cimbi-36	2.0 [8.69 ± 0.28] 80 ± 4	11 [7.94 ± 0.13] 110 ± 5	0.12 [10.04 ± 0.19] 81 ± 4 $^{(4)}$	12 [7.94 ± 0.08] 109 ± 3 $^{(3)}$
25CN-NBOH (compound 1)	2.1 [8.68 ± 0.05] 86 ± 12	170 [6.76 ± 0.13] 86 ± 11	2.4 [8.62 ± 0.14] 77 ± 5 $^{(4)}$	350 [6.45 ± 0.06] 114 ± 3 $^{(4)}$
25CN-NBOMe (compound 2)	3.5 [8.46 ± 0.10] 86 ± 2	130 [6.87 ± 0.10] 91 ± 3	3.7 [8.43 ± 0.03] 85 ± 4 $^{(3)}$	230 [6.63 ± 0.08] 101 ± 8 $^{(3)}$
25CN-NBF (compound 3)	81 [7.09 ± 0.06] 70 ± 4	1,400 [5.85 ± 0.05] 79 ± 6	130 [6.90 ± 0.15] 61 ± 4 $^{(3)}$	3,600 [5.44 ± 0.12] 83 ± 7 $^{(3)}$
25CN-NBMD (compound 4)	19 [7.72 ± 0.12] 84 ± 4	1,500 [5.81 ± 0.09] 72 ± 3	30 [7.53 ± 0.11] 70 ± 3 $^{(3)}$	3,500 [5.46 ± 0.14] 57 ± 9 $^{(3)}$

n.t., not tested.

[a]The data for the [^{3}H]IP$_{1\text{-}3}$ assay have been published previously, the data for 5-HT and DOI are given in Hansen et al. (2015) and the data for the other compounds are given in Hansen et al. (2014).

compounds in the IP-One assay were also in concordance with those determined for the agonists in the IP turnover assay (Table 3).

Next, the functional properties of the four analogs, DOI, and a couple of other reference 5-HT$_2$R agonists were characterized at human 5-HT$_{2A}$R, 5-HT$_{2B}$R, and 5-HT$_{2C}$R in two fluorescence-based Ca^{2+} imaging assays (Ca^{2+} assays I and II). Analogous to the IP assays, the functional readout in these assays is a reflection of Gα_q-mediated receptor signaling (measured further downstream in the signaling cascade). However, in contrast to the IP assays the functional responses in the Ca^{2+} assay are recorded in real time and not as endpoint measurements. Moreover, although the two Ca^{2+} assay protocols used in this study were essentially identical, the assays were performed using different 5-HT$_{2A}$R-, 5-HT$_{2B}$R-, and 5-HT$_{2C}$R-expressing cell lines and in different laboratories, and thus the two data sets for the compounds from these assays serve to probe the importance of these differences for the functional properties displayed by the agonists. In previous studies we have found the functional properties exhibited by the three 5-HT$_2$Rs in both combinations of cell lines and assays to be in good agreement with the literature data for the receptors (Jensen et al., 2013; Cheng et al., 2016).

The rank orders of agonist potencies displayed by DOI and the four analogs at 5-HT$_{2A}$R and 5-HT$_{2C}$R were the same in the two Ca^{2+} assays, and these were also the same as in the two IP assays: DOI ~ 25CN-NBOH ~ 25CN-NBOMe > 25CN-NBMD > 25CN-NBF for 5-HT$_{2A}$R and DOI ~ 25CN-NBOH ~ 25CN-NBOMe > 25CN-NBMD ~ 25CN-NBF for 5-HT$_{2C}$R (Fig. 3B; Table 4). Importantly, analogous to their functional profiles in the IP assays, 25CN-NBOH and 25CN-NBMD were substantially more selective for 5-HT$_{2A}$R over 5-HT$_{2C}$R than DOI in both Ca^{2+} assays (Figs. 3 and 4B; Tables 3 and 4). Moreover, the rank order of agonist potencies displayed by DOI and the four analogs at a 5-HT$_{2B}$R-expressing cell line in Ca^{2+} assay I (DOI ~ 25CN-NBOMe > 25CN-NBOH > 25CN-NBMD > 25CN-NBF) was also in fairly good agreement with their binding affinities in the [^{3}H]LSD binding assay. The EC_{50} values exhibited by the five agonists at this receptor were very similar to those at 5-HT$_{2C}$R in this assay, and thus 25CN-NBOH and 25CN-NBMD were also substantially more selective for 5-HT$_{2A}$R over 5-HT$_{2B}$R than DOI (Table 4). Finally, the intrinsic activities displayed by DOI and the four analogs at the two receptors in the two Ca^{2+} assays were also very comparable to those obtained in the IP assays. All four analogs were partial agonists at 5-HT$_{2A}$R (R_{max} values of 54%–87%) and 5-HT$_{2B}$R (R_{max} values of 24%–79%), whereas 25CN-NBOH and 25CN-NBOMe were full agonists (R_{max} values of 93%–100%) and 25CN-NBF and 25CN-NBMD were partial agonists (R_{max} values of 28%–84%) at 5-HT$_{2C}$R (Table 4).

5-HT$_{2A}$R Selectivities of DOI and the Four Analogs in the Binding and Functional Assays

In Fig. 4, the degrees of 5-HT$_{2A}$R-over-5-HT$_{2B}$R and 5-HT$_{2A}$R-over-5-HT$_{2C}$R selectivities exhibited by DOI and the four analogs against the binding affinity in the radioligand binding assays and the relative activity [$\Delta\log(R_{max}/EC_{50})$] in the functional assays are given. In terms of binding affinity, all four analogs generally displayed substantially higher 5-HT$_{2A}$R-over-5-HT$_{2C}$R selectivity compared with DOI, the rank order of selectivity being 25CN-NBMD > 25CN-NBOH > 25CN-NBOMe > 25CN-NBF (Fig. 4A; Table 1). Analogously, all four analogs showed higher 5-HT$_{2A}$R-over-5-HT$_{2B}$R selectivity compared with DOI in the [^{3}H]LSD assay, with the rank order of 25CN-NBOH ~ 25CN-NBMD > 25CN-NBOMe > 25CN-NBF (Fig. 4B).

Since all four analogs and DOI exhibited agonist activity at all three 5-HT$_2$R subtypes, comparing the functional activity at each of these receptors can be used to estimate their

TABLE 4

Agonist properties displayed by 5-HT, DOI, 25I-NBOMe, Cimbi-36, and compounds 1–4 at human 5-HT_{2A}R, 5-HT_{2B}R, and 5-HT_{2C}R expressed in mammalian cell lines in fluorescence-based Ca^{2+} assays I and II

The two Ca^{2+} assays were performed as described in *Materials and Methods*. The EC_{50} values are given in nM with the pEC_{50} ± S.E.M. values in brackets and the R_{max} ± S.E.M. values given as the percentage of the maximal response induced by 5-HT. The number of experiments (n) for each set of potency and efficacy data are given in superscript.

	Ca^{2+} Assay I			Ca^{2+} Assay II[a]	
	5-HT_{2A}R	5-HT_{2B}R	5-HT_{2C}R	5-HT_{2A}R	5-HT_{2C}R
	EC_{50} [EC_{50} ± S.E.M.] R_{max} ± S.E.M.$^{(n)}$	EC_{50} [EC_{50} ± S.E.M.] R_{max} ± S.E.M.$^{(n)}$	EC_{50} [EC_{50} ± S.E.M.] R_{max} ± S.E.M.$^{(n)}$	EC_{50} [EC_{50} ± S.E.M.] R_{max} ± S.E.M.$^{(n)}$	EC_{50} [EC_{50} ± S.E.M.] R_{max} ± S.E.M.$^{(n)}$
5-HT	0.61 [9.22 ± 0.03] 100 $^{(5)}$	0.72 [9.14 ± 0.03] 100 $^{(5)}$	0.30 [9.52 ± 0.03] 100 $^{(5)}$	1.0 [9.01 ± 0.06] 100 $^{(6)}$	1.3 [8.89 ± 0.05] 100 $^{(6)}$
DOI	0.85 [9.07 ± 0.04] 91 ± 1 $^{(4)}$	2.0 [8.69 ± 0.03] 94 ± 1 $^{(3)}$	3.3 [8.48 ± 0.04] 96 ± 1 $^{(4)}$	0.15 [9.81 ± 0.06] 85 ± 2 $^{(4)}$	6.6 [8.18 ± 0.10] 85 ± 3 $^{(4)}$
25I-NBOMe	0.44 [9.35 ± 0.05] 86 ± 2 $^{(3)}$	8.9 [8.05 ± 0.06] 80 ± 2 $^{(3)}$	1.1 [8.95 ± 0.03] 96 ± 1 $^{(5)}$	n.t.	n.t.
Cimbi-36 [a]	1.6 [8.80 ± 0.05] 88 ± 1 $^{(3)}$	7.3 [8.13 ± 0.04] 79 ± 1 $^{(3)}$	0.98 [9.01 ± 0.04] 97 ± 2 $^{(4)}$	0.95 [9.02 ± 0.09] 83 ± 3 $^{(4)}$	0.90 [9.04 ± 0.06] 99 ± 7 $^{(4)}$
25CN-NBOH (compound 1)	1.2 [8.92 ± 0.04] 77 ± 5 $^{(4)}$	59 [7.23 ± 0.05] 60 ± 2 $^{(3)}$	23 [7.65 ± 0.03] 99 ± 1 $^{(3)}$	0.41 [9.39 ± 0.10] 80 ± 4 $^{(4)}$	52 [7.28 ± 0.07] 93 ± 2 $^{(5)}$
25CN-NBOMe (compound 2)	1.2 [8.91 ± 0.04] 87 ± 1 $^{(3)}$	12 [7.93 ± 0.03] 79 ± 1 $^{(3)}$	9.3 [8.03 ± 0.03] 100 ± 1 $^{(3)}$	0.40 [9.40 ± 0.10] 81 ± 5 $^{(3)}$	36 [7.44 ± 0.08] 96 ± 3 $^{(5)}$
25CN-NBF (compound 3)	17 [7.78 ± 0.03] 82 ± 1 $^{(3)}$	940 [6.03 ± 0.14] 24 ± 3 $^{(3)}$	460 [6.34 ± 0.06] 84 ± 3 $^{(3)}$	32 [7.50 ± 0.02] 54 ± 5 $^{(4)}$	580 [6.24 ± 0.05] 50 ± 5 $^{(6)}$
25CN-NBMD (compound 4)	5.6 [8.25 ± 0.03] 83 ± 1 $^{(5)}$	220 [6.65 ± 0.13] 31 ± 2 $^{(4)}$	480 [6.32 ± 0.07] 71 ± 3 $^{(5)}$	5.8 [8.23 ± 0.12] 56 ± 6 $^{(4)}$	570 [6.24 ± 0.05] 28 ± 4 $^{(5)}$

n.t., not tested.
[a]The data for Cimbi-36 in Ca^{2+} assay II have been published previously (Herth et al., 2016).

functional 5-HT_{2A}R selectivity. While potency ratios of full agonists are independent of receptor density and efficiency of coupling effects, the same is not true when comparing the relative potency of partial agonists because changes in assay sensitivity produce effects of different magnitude to full versus partial agonists (Kenakin et al., 2012). Using calculated $\Delta\log(R_{max}/EC_{50})$ values and 5-HT as references to measure 5-HT_{2A}R selectivity, all four analogs exhibited substantial 5-HT_{2A}R-over-5-HT_{2C}R selectivity across functional assays with the general rank order of 25CN-NBMD > 25CN-NBOH > 25CN-NBOMe > 25CN-NBF (Fig. 4C). 25CN-NBOH and 25CN-NBMD displayed significantly higher 5-HT_{2A}R-over-5-HT_{2C}R selectivities than DOI in all of the functional assays, with 25CN-NBMD exhibiting greater than 150-fold 5-HT_{2A}R selectivity in all four assays interrogated (Fig. 4C). The 5-HT_{2A}R-over-5-HT_{2B}R selectivities displayed by the four analogs and DOI in Ca^{2+} assay I were also examined using $\Delta\log(R_{max}/EC_{50})$ values, and all four analogs displayed considerably higher 5-HT_{2A}R selectivities than DOI, the rank order being 25CN-NBF > 25CN-NBMD > 25CN-NBOH > 25CN-NBOMe (Fig. 4D).

Screening of 25CN-NBOH at Other Putative Molecular Targets

The possible existence of other targets for 25CN-NBOH than the 5-HT_2Rs was investigated in comprehensive screens of the compound (at an assay concentration of 10 μM) at a plethora of neurotransmitter receptors and transporters, ion channels, and enzymes in radioligand binding assays and at a broad spectrum of kinases and other enzymes in enzyme assays. The complete data sets from these screens are given in Supplemental Table 1, and the targets where 25CN-NBOH (10 μM) displayed significant activity are summarized in Table 5. In addition to its nanomolar binding affinities to the three 5-HT_2R subtypes, 25CN-NBOH also displayed appreciable binding affinity at 5-HT_6 (K_i value of 310 nM), dopamine D_4 (K_i value 2.9 μM), α_{2A}, α_{2B}, and α_{2C} adrenergic (K_i values of 1.2–2.9 μM), H_1 histamine (K_i value of 2.1 μM), κ opioid (K_i value of 4.2 μM), and sigma-1 and -2 (K_i values of 120–280 nM) receptors. 25CN-NBOH (10 μM) also inhibited radioligand binding to other targets by approximately 50%, thus displaying estimated IC_{50} values of 10 μM at these targets (Supplemental Table 1). However, the compound was inactive at the majority of targets included in the radioligand binding screening. Finally, 25CN-NBOH was also tested at a wide range of kinases and other enzymes in enzymatic assays, displaying no significant activity at any of these at an assay concentration of 10 μM (Supplemental Table 1). In addition, we found that 25CN-NBOH inhibited hERG with an IC_{50} value of 2.7 μM.

It is important to stress that lack of inhibition of radioligand binding to a specific target in these assays not necessarily reflects inactivity of the test compound at the target since the compound potentially could bind to a site distinct from the site targeted by the radioligand without affecting its binding. However, the majority of targets assayed by radioligand binding in the screening were class A GPCRs, and considering that few allosteric ligands of these receptors have been reported not to affect orthosteric radioligand binding (Keov et al., 2011) we propose that these receptor binding data are likely to be highly predictive of the functional activity of 25CN-NBOH at these targets. Moreover, 25CN-NBOH would be expected to most likely act through the orthosteric sites of the monoaminergic and muscarinic acetylcholine receptors included in this screening, and thus its ability to compete with orthosteric radioligands for binding is a direct measurement of its activity at these receptors.

Solubility

The solubility of 25CN-NBOH at pH 7.4 was determined to be 405 μg/ml. However, we have been able to make stock solution for in vivo investigation with concentrations up to 3 mg/ml in physiologic saline (0.9% NaCl) by sonication and where up to

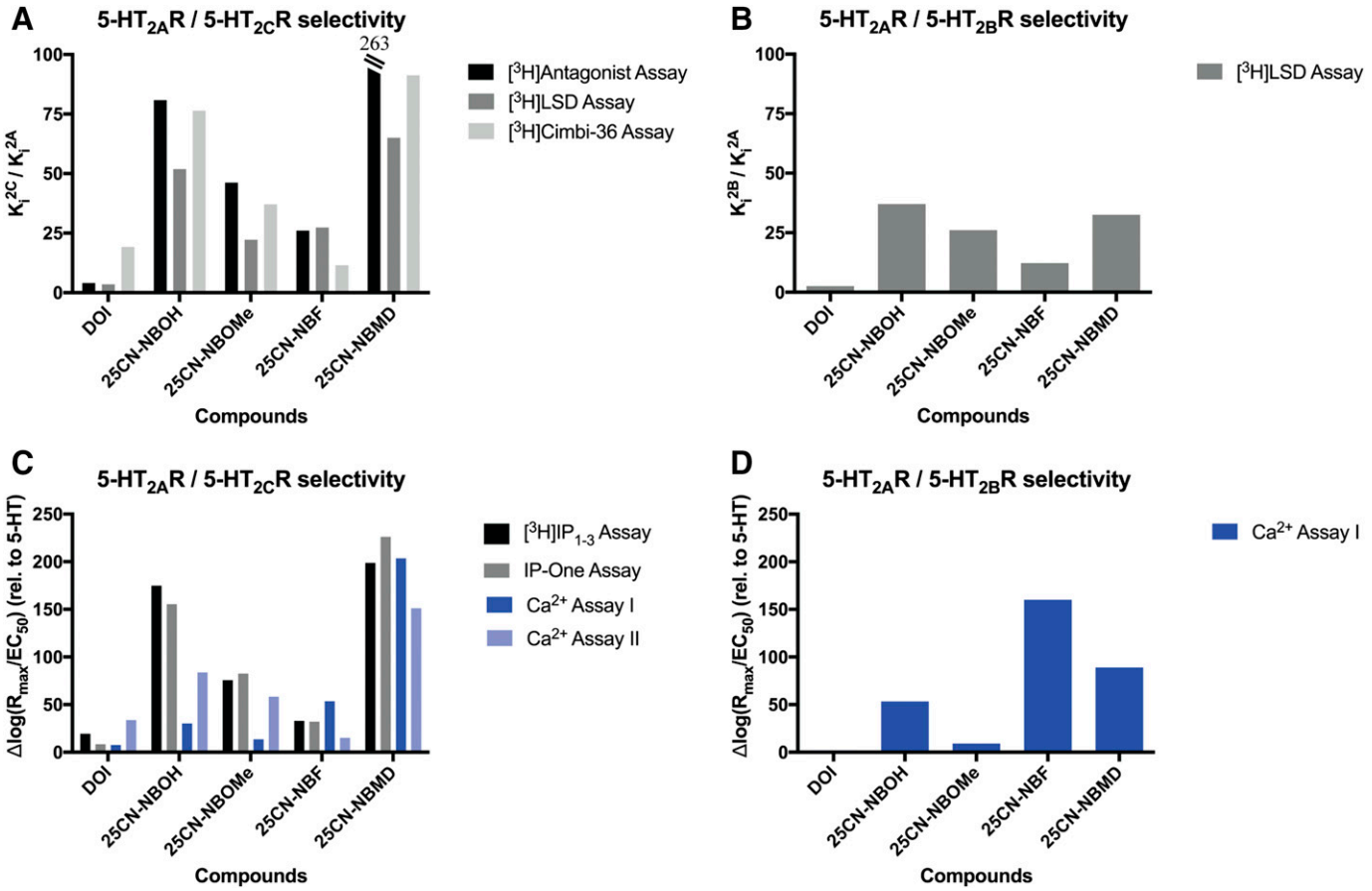

Fig. 4. Subtype-selectivity profiles of DOI, 25CN-NBOH, 25CN-NBOMe, 25CN-NBF, and 25CN-NBMD at human 5-HT$_2$Rs in the binding and functional assays. (A) The K_i^{2C}/K_i^{2A} ratios determined for the five agonists at 5-HT$_{2A}$R and 5-HT$_{2C}$R in the [^{3}H]antagonist (5-HT$_{2A}$R: [^{3}H]ketanserin; 5-HT$_{2C}$R: [^{3}H]mesulergine), [^{3}H]LSD, and [^{3}H]Cimbi-36 competition binding assays. (B) The K_i^{2B}/K_i^{2A} ratios determined for the five agonists at 5-HT$_{2A}$R and 5-HT$_{2B}$R in the [^{3}H]LSD competition binding assay. (C) The $\Delta\log(R_{max}/EC_{50})$ values (relative to 5-HT) for the five agonists at 5-HT$_{2A}$R and 5-HT$_{2C}$R in the functional [^{3}H]IP$_{1\text{-}3}$, IP-One and Ca^{2+} assays I and II. (D) The $\Delta\log(R_{max}/EC_{50})$ values (relative to 5-HT) for the five agonists at 5-HT$_{2A}$R and 5-HT$_{2B}$R in the Ca^{2+} assay I.

5 mg/ml if 5% dimethylsulfoxide was added. Upon storage at 5°C some precipitation was seen but sonication caused the compound to redissolve. 25CN-NBOH is stable for at least several weeks when stored and handled in this way as judged by liquid chromatography/mass spectrometry analysis at various time points.

Toxicology Screening

In the high-content screening of 25CN-NBOH for acute cellular toxicity, no effects were seen for 25CN-NBOH at any of the six parameters tested (nuclei counts, nuclear area, plasma membrane integrity, lysosomal activity, mitochondrial membrane potential, and mitochondrial area) at concentrations up to 100 μM, indicating a very benign cellular toxicological profile.

Pharmacokinetic Properties of 25CN-NBOH

To assess the blood-brain barrier permeability of 25CN-NBOH, the compound was tested in the MDCK assay. In this assay, 25CN-NBOH displayed high bidirectional permeability (apical-basal 29 $\pm$ 1.1 cm/s $\times$ 10^{-6}; basal-apical 20 $\pm$ 2.2 cm/s $\times$ 10^{-6}), and the resulting efflux ratio of 0.71 $\pm$ 0.05 indicated lack of involvement of P-glycoprotein-mediated transport. 25CN-NBOH was found to be highly unstable in the presence of murine microsomes, with a MCL_{int} of 260 l/kg/h.

To investigate the in vivo exposure of 25CN-NBOH in mice and the correlation between the free unbound concentrations of the drug in the brain and its in vivo efficiency, 25CN-NBOH (3 mg/kg, s.c.) was administered to C57BL/6 mice mice, and plasma and brain exposure of the drug was determined after 5, 15, and 30 minutes. The design of the study in terms of the drug dose, administration route, and mouse strain used in the experiments was partly rooted in our wish to be able to approximate the drug exposure in mice receiving this dose in the Halberstadt et al. (2016) study. Thus, the time points for the analysis were chosen based on the 5-minute period between administration and the start of testing in that study. The good in vitro transport characteristics exhibited by 25CN-NBOH in the MDCK assay was reflected in this study since 25CN-NBOH was found to rapidly penetrate the blood-brain barrier (Fig. 5). By combining the free fractions of the compound determined in plasma (18% $\pm$ 1.3%) and brain (4.0% $\pm$ 0.2%), the unbound concentrations of 25CN-NBOH were calculated and found to be comparable in plasma and brain, suggesting an unrestricted passage across the blood-brain barrier with rapid attainment of equilibrium between the compartments. The unbound brain concentration of 25CN-NBOH reached approximately 200 nM only 15 minutes after administration of the 3 mg/kg dose and remained at this level until 30 minutes after the administration (Fig. 5B).

Discussion

The overall conclusion from the elaborate in vitro pharmacological characterization of 25CN-NBOH at human 5-HT$_2$Rs

TABLE 5

Pharmacological properties displayed by 25CN-NBOH (compound 1) at selected receptor targets in radioligand binding assays

The data for the receptor are from broad profiling screens performed at Eurofins and PDSP. The data included in the table are for receptors in these screens where 25CN-NBOH (10 μM) exhibited significant inhibition, and where a K_i or an IC_{50} value thus could be estimated. The complete data sets for the screens are given in Supplemental Table 1. The inhibition mediated by 25CN-NBOH (10 μM) in competition binding assays to the receptors are given in percentages (positive and negative values representing percentage of inhibition and percentage of potentiation relative to control, respectively) with the estimated K_i or IC_{50} values. The data are given as the mean values based on two independent determinations.

Target	Assay/Radioligand	Inhibition at 10 μM	K_i/IC_{50}
			μM
5-HT_{2A} (h), E	[^{125}I](±)DOI$^{(ago)}$	98	<10
5-HT_{2A} (h), P	[^{3}H]Ketanserin$^{(anta)}$	>50	0.0032
5-HT_{2B} (h), E	[^{125}I](±)DOI$^{(ago)}$	104	<10
5-HT_{2B} (h), P	[^{3}H]LSD$^{(ago)}$	>50	0.075
5-HT_{2C} (h), E	[^{125}I](±)DOI$^{(ago)}$	101	<10
5-HT_{2C} (h), P	[[^{3}H]Mesulergine$^{(anta)}$	>50	0.056
5-HT_{6} (h), P	[^{3}H]LSD$^{(ago)}$	>50	0.31
D_4 (h), P	[^{3}H]methyl-spiperone$^{(anta)}$	>50	2.9
α_{2A} (h), P	[^{3}H]Rauwolscine$^{(anta)}$	>50	1.2
α_{2B} (h), P	[^{3}H]Rauwolscine$^{(anta)}$)	>50	2.0
α_{2C} (h), P	[^{3}H]Rauwolscine$^{(anta)}$	>50	2.9
H_1 (h), P	[^{3}H]pyrilamine$^{(anta)}$	>50	2.1
Opioid κ (h), P	[^{3}H]U69593$^{(ago)}$	>50	4.2
Sigma-1 (rat brain), P	[^{3}H]Pentazocine(+)	>50	0.28
Sigma-2 (PC12, rat), P	[^{3}H]DTG$^{(ago)}$	>50	0.12

ago, agonist; anta, antagonist; E, Eurofins; h, human; P, Psychoactive Drug Screening Program.

in the various binding and functional assays in this study is that the compound is a highly selective 5-HT_{2A}R agonist. 25CN-NBOH displayed high-picomolar/low-nanomolar binding affinities and functional potencies at 5-HT_{2A}R, and its selectivity for 5-HT_{2A}R over the other 5-HT_2R subtypes is reflected in the K_i^{2B}/K_i^{2A} and K_i^{2C}/K_i^{2A} ratios derived from the binding assays and in the $\log[R_{max}/EC_{50}]$ values derived from the functional data (Fig. 4). The different degrees of 5-HT_{2A}R-over-5-HT_{2C}R selectivity exhibited by 25CN-NBOH in these assays are not particularly surprising, since absolute binding affinities and potencies of GPCR agonists in these assays are known to be highly dependent on both experimental conditions and receptor/G protein expression levels and stoichiometries in the cells (Bräuner-Osborne et al., 1996). Along the same lines, the extent to which the pronounced 5-HT_{2A}R selectivity exhibited by 25CN-NBOH at recombinant receptors is translated into subtype selectivity in vivo remains to be investigated, since environmental factors and expression levels of 5-HT_2Rs and their effector proteins in native tissue are likely to be very different from those in the in vitro assays. It should also be stressed that the functional properties of 25CN-NBOH at three 5-HT_2Rs in the present study exclusively were investigated in assays measuring Gα_q-mediated signaling, and it thus remains to be seen whether the drug exhibits similar degrees of 5-HT_{2A}R selectivity when it comes to the G protein-independent signaling mediated by the 5-HT_2Rs (McCorvy and Roth, 2015; Maroteaux et al., 2017). Thus, the strongest case for the 5-HT_{2A}R selectivity of 25CN-NBOH presently is the consistently higher selectivity of it compared with DOI in all binding and functional assays in this study (Fig. 4).

The detailed pharmacological profiling of 25CN-NBOH and the three other *N*-benzyl-2,5-dimethoxy-4-cyanophenylethylamine analogs at the 5-HT_2Rs also offers interesting structure-activity relationship observations. The importance of the identity of the 2′-substituent for the functional properties of the four analogs, both their overall binding affinity/agonist potency across the three receptors and their 5-HT_2R-selectivity profiles, is quite remarkable. The fact that the 2′-fluoro-substituted analog (25CN-NBF) is the least potent of the four analogs (Tables 1–4) suggests that the presence of an oxygen in the 2′-substituent is a key determinant of high-affinity 5-HT_2R binding. As for the three other analogs, it is interesting that while the replacement of the 2′-hydroxy-substituent in 25CN-NBOH with a methoxy group (25CN-NBOMe) is well tolerated, introduction of the 2′,3′-methylenedioxy moiety is detrimental for binding affinity and functional potency of the scaffold at all three 5-HT_2Rs. It seems that the increased bulkiness of the substituent in 25CN-NBMD either poses a steric clash with residues in the orthosteric binding site or that the incorporation of the oxygen into a ring system impairs the ability of the atom to form an interaction with the receptor. On the other hand, it is noteworthy that 25CN-NBMD exhibits comparable, and in some assays even superior, selectivity for 5-HT_{2A}R over 5-HT_{2B}R and 5-HT_{2C}R compared with 25CN-NBOH. While 25CN-NBOH clearly is more suited as a pharmacological tool because of its higher potency, 25CN-NBMD could thus be an interesting lead for future development of potent 5-HT_{2A}R-selective agonists, in particular if its reduced binding affinity is rooted in a different spatial orientation of the compound in the binding pocket than 25CN-NBOH.

To assess the global selectivity profile of 25CN-NBOH, the compound (10 μM) was subjected to an elaborate screening at a plethora of other putative targets in radioligand binding and enzyme assays (Supplemental Table 1; Table 5). There was a considerable overlap between targets assayed in the Eurofins and the National Institute of Mental Health's Psychoactive Drug Screening Program screenings, and for these targets only a few insignificant differences were observed between the two data sets. The screening results were also in good agreement with data reported for the compound (screened at a concentration of 1 μM by the National Institute of Mental Health's Psychoactive Drug Screening Program) in a recent study, the only substantial differences between the two data sets being the

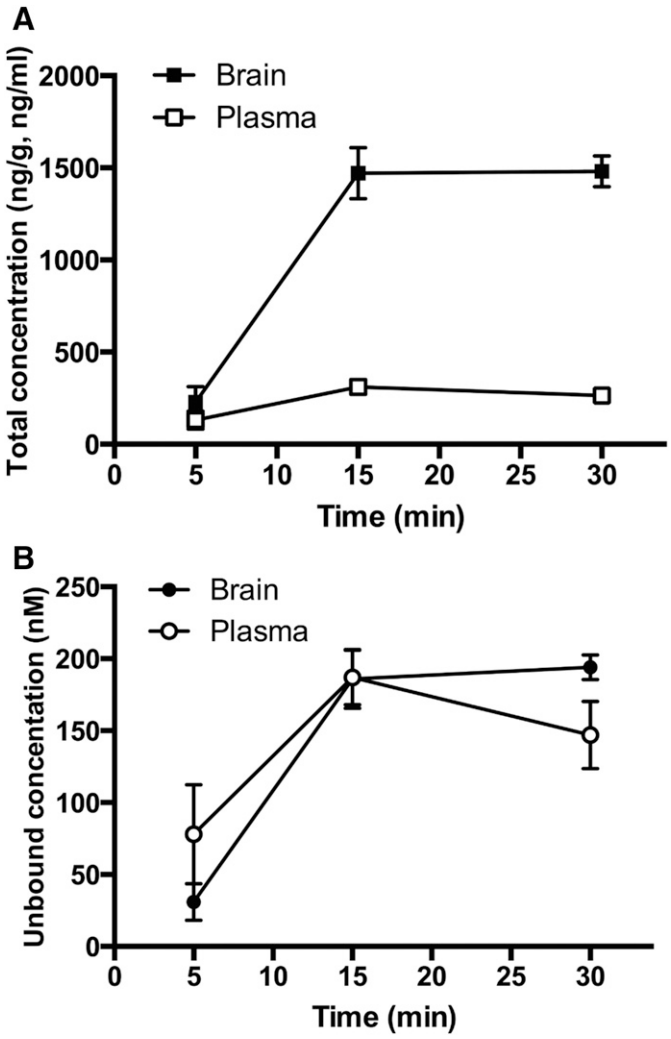

Fig. 5. Brain and plasma concentrations of 25CN-NBOH in C57BL/6 mice following subcutaneous administration of 3 mg/kg. Data are shown as mean ± S.D. (n = 3/time point) expressed as total concentrations (A) and unbound 25CN-NBOH concentrations calculated from the total concentrations and the free fractions determined for the compound (B). In (A), total concentrations of 25CN-NBOH in brain and plasma are given in ng/g and ng/ml, respectively.

observed activity of 25CN-NBOH at H_2 histamine (K_i value of 674 nM) and β_2 adrenergic (K_i value of 720 nM) receptors reported by Halberstadt et al. (2016), which contrast the inactivity of the compound at these receptors in this study ($IC_{50} > 10\ \mu M$). Regardless of which of these values are correct, 25CN-NBOH displayed ≥100-fold higher binding affinities to 5-HT$_{2A}$R than to all non-5-HT$_2$R targets in the screening, and thus the compound seems to be highly selective for 5-HT$_2$Rs, and in particular for 5-HT$_{2A}$R.

The pharmacokinetic characteristics displayed by 25CN-NBOH combined with the levels of brain exposure of the drug following systemic administration in mice suggest that the compound is well suited as a pharmacological tool in in vivo studies of 5-HT$_{2A}$Rs. 25CN-NBOH was found to rapidly cross the cellular barrier and not to be a substrate for P-glycoprotein-mediated efflux in MDCK-MDR1 monolayers, a well-established in vitro model of the blood-brain barrier (Feng et al., 2008). Based on its high murine intrinsic clearance (MCL_{int}) we expected 25CN-NBOH to be cleared extremely fast in vivo, even with s.c. dosing; however, our in vivo exposure study showed that 25CN-NBOH (3 mg/kg, s.c.) rapidly reached the CNS yielding a high-nanomolar concentration of the unbound drug that was fairly stable over time, at least until 30 minutes after administration (Fig. 5B).

While the rapid exposure of the high levels of free 25CN-NBOH in the brain following systemic administration demonstrates the feasibility of using the agonist for in vivo studies, it also raises the question of what the optimal dose range for 25CN-NBOH in such studies would be. 25CN-NBOH has been applied in two recent in vivo studies, where Halberstadt et al. (2016) used doses ranging from 0.3 to 6 mg/kg s.c. in C57BL/6J mice and Fantegrossi et al. (2015) used doses ranging from 0.1 to 30 mg/kg i.p. in NIH Swiss mice. However, since neither of the two studies determined the brain exposure levels of the drug arising from these doses, the levels of 5-HT$_{2A}$R activation underlying its behavioral effects were not addressed (Fantegrossi et al., 2015; Halberstadt et al., 2016). Our exposure study was partly designed to approximate the experimental conditions used by Halberstadt et al. (2016), but more importantly we wanted overall insight into the correlation between 25CN-NBOH dosing and the resulting brain exposure of the free drug. 25CN-NBOH (3 mg/kg, s.c.) produced rapidly increasing concentrations of free drug in mice brains, peaking at ~200 nM after 15 minutes and remaining at this level for some time (Fig. 5B). It should be noted that the determined levels of free 25CN-NBOH are global concentrations, and thus it is possible that the drug could be differentially distributed throughout the brain. Moreover, caution should be taken when extrapolating from these exposure data to the levels of 5-HT$_2$R activation mediated by 25CN-NBOH in vivo since the EC_{50} values exhibited by 25CN-NBOH at the recombinant human 5-HT$_2$Rs are not necessarily representative of its potencies at the native murine 5-HT$_2$Rs. Nevertheless, while keeping these reservations in mind, a 25CN-NBOH concentration of 200 nM would be expected to activate 5-HT$_{2A}$Rs completely, but it could also mediate significant activation of the two other 5-HT$_2$R subtypes (Tables 3 and 4). Analogously, although the use of a different administration route and a different mouse strain in the Fantegrossi et al. (2015) study complicates interpretations even further, it is reasonable to speculate that 25CN-NBOH concomitantly with its 5-HT$_{2A}$R stimulation could mediate significant activation of 5-HT$_{2B}$R and 5-HT$_{2C}$R at some point in the 0.1–30 mg/kg (i.p.) dose range used in this study. Thus, even though the separation between 5-HT$_{2A}$R- and 5-HT$_{2B}$R/5-HT$_{2C}$R-effective concentrations clearly is bigger for 25CN-NBOH than for DOI, the dosing of 25CN-NBOH in in vivo studies focused on delineating 5-HT$_{2A}$R functions could still be a balance between obtaining sufficient 5-HT$_{2A}$R activation while keeping concomitant activation of the other 5-HT$_2$Rs to a minimum.

As mentioned in the *Introduction*, there is an increasing interest in psychedelics and 5-HT$_{2A}$R agonists as putative therapeutics, not only when it comes to numerous psychiatric disorders but also for the treatment of addiction and alcoholism, cluster head aches, and various inflammatory disorders (Sewell et al., 2006; Yu et al., 2008; Nau et al., 2013, 2015; Hendricks et al., 2014; Johnson et al., 2014; Bogenschutz et al., 2015; Nichols, 2016). Although there is little doubt that 5-HT$_{2A}$R is the main mediator of these in vivo effects, the agonist properties exhibited by these drugs at 5-HT$_{2B}$R, 5-HT$_{2C}$R, and other 5-HT receptors on the other hand suggest that additional receptors could be activated to some degree

within the 5-HT_{2A}R-effective concentration range and thus potentially contribute to the observed effects. While these putative contributions in previous studies have been assessed by coapplication of 5-HT_{2A}R agonists with various subtype-selective antagonists of other 5-HT receptor subtypes, a truly 5-HT_{2A}R-specific agonist would be an interesting pharmacological tool for studies of native 5-HT_{2A}R signaling. Although 25CN-NBOH admittedly cannot be considered a completely 5-HT_{2A}R-specific agonist, we propose that its superior 5-HT_{2A}R selectivity compared with DOI, its high brain uptake, and its benign acute cellular toxicological profile make it a valuable tool for explorations of the physiologic functions of and the therapeutic potential in these receptors.

Acknowledgments

Some of the in vitro binding data for 25CN-NBOH were generously provided by the National Institute of Mental Health's Psychoactive Drug Screening Program (NIMH PDSP), Contract No. HHSN-271-2008-025C. The NIMH PDSP is directed by Bryan L. Roth at the University of North Carolina (Chapel Hill, NC) and project officer Jamie Driscol at NIMH (Bethesda, MD).

Authorship Contributions

Participated in research design: Jensen, McCorvy, Leth-Petersen, Bundgaard, Bräuner-Osborne, Kehler, Kristensen.

Conducted experiments: Jensen, McCorvy, Bundgaard, Liebscher.

Contributed new reagents or analytic tools: Leth-Petersen, Kristensen.

Performed data analysis: Jensen, McCorvy, Leth-Petersen, Bundgaard, Liebscher, Kenakin, Bräuner-Osborne, Kehler, Kristensen.

Wrote or contributed to the writing of the manuscript: Jensen, McCorvy, Leth-Petersen, Bundgaard, Liebscher, Kenakin, Bräuner-Osborne, Kehler, Kristensen.

References

Almaula N, Ebersole BJ, Ballesteros JA, Weinstein H, and Sealfon SC (1996) Contribution of a helix 5 locus to selectivity of hallucinogenic and nonhallucinogenic ligands for the human 5-hydroxytryptamine2A and 5-hydroxytryptamine2C receptors: direct and indirect effects on ligand affinity mediated by the same locus. *Mol Pharmacol* **50**:34–42.

Berger M, Gray JA, and Roth BL (2009) The expanded biology of serotonin. *Annu Rev Med* **60**:355–366.

Besnard J, Ruda GF, Setola V, Abecassis K, Rodriguiz RM, Huang XP, Norval S, Sassano MF, Shin AI, Webster LA, et al. (2012) Automated design of ligands to polypharmacological profiles. *Nature* **492**:215–220.

Black JW and Leff P (1983) Operational models of pharmacological agonism. *Proc R Soc Lond B Biol Sci* **220**:141–162.

Black JW, Leff P, Shankley NP, and Wood J (1985) An operational model of pharmacological agonism: the effect of E/[A] curve shape on agonist dissociation constant estimation. *Br J Pharmacol* **84**:561–571.

Bogenschutz MP, Forcehimes AA, Pommy JA, Wilcox CE, Barbosa PC, and Strassman RJ (2015) Psilocybin-assisted treatment for alcohol dependence: a proof-of-concept study. *J Psychopharmacol* **29**:289–299.

Bräuner-Osborne H, Ebert B, Brann MR, Falch E, and Krogsgaard-Larsen P (1996) Functional partial agonism at cloned human muscarinic acetylcholine receptors. *Eur J Pharmacol* **313**:145–150.

Canal CE, Booth RG, and Morgan D (2013) Support for 5-HT2C receptor functional selectivity in vivo utilizing structurally diverse, selective 5-HT2C receptor ligands and the 2,5-dimethoxy-4-iodoamphetamine elicited head-twitch response model. *Neuropharmacology* **70**:112–121.

Carhart-Harris RL, Bolstridge M, Rucker J, Day CM, Erritzoe D, Kaelen M, Bloomfield M, Rickard JA, Forbes B, Feilding A, et al. (2016) Psilocybin with psychological support for treatment-resistant depression: an open-label feasibility study. *Lancet Psychiatry* **3**:619–627.

Celada P, Puig M, Amargós-Bosch M, Adell A, and Artigas F (2004) The therapeutic role of 5-HT_{1A} and 5-HT_{2A} receptors in depression. *J Psychiatry Neurosci* **29**:252–265.

Cheng J, McCorvy JD, Giguere PM, Zhu H, Kenakin T, Roth BL, and Kozikowski AP (2016). Design and discovery of functionally selective serotonin 2C (5-HT_{2C}) receptor agonists. *J Med Chem* **59**:9866–9880.

Fantegrossi WE, Gray BW, Bailey JM, Smith DA, Hansen M, and Kristensen JL (2015) Hallucinogen-like effects of 2-([2-(4-cyano-2,5-dimethoxyphenyl) ethylamino]methyl)phenol (25CN-NBOH), a novel *N*-benzylphenethylamine with 100-fold selectivity for 5-HT_{2A} receptors, in mice. *Psychopharmacology (Berl)* **232**:1039–1047.

Feng B, Mills JB, Davidson RE, Mireles RJ, Janiszewski JS, Troutman MD, and de Morais SM (2008) In vitro P-glycoprotein assays to predict the in vivo interactions of P-glycoprotein with drugs in the central nervous system. *Drug Metab Dispos* **36**: 268–275.

González-Maeso J and Sealfon SC (2009) Psychedelics and schizophrenia. *Trends Neurosci* **32**:225–232.

Halberstadt AL (2015) Recent advances in the neuropsychopharmacology of serotonergic hallucinogens. *Behav Brain Res* **277**:99–120.

Halberstadt AL, Sindhunata IS, Scheffers K, Flynn AD, Sharp RF, Geyer MA, and Young JW (2016) Effect of 5-HT_{2A} and 5-HT_{2C} receptors on temporal discrimination by mice. *Neuropharmacology* **107**:364–375.

Hannon J and Hoyer D (2008) Molecular biology of 5-HT receptors. *Behav Brain Res* **195**:198–213.

Hansen M, Jacobsen SE, Plunkett S, Liebscher GE, McCorvy JD, Bräuner-Osborne H, and Kristensen JL (2014) Synthesis and structure-activity relationships of *N*-benzyl phenethylamines as 5-$HT_{2A/2C}$ agonists. *ACS Chem Neurosci* **5**:243–249.

Hansen M, Jacobsen SE, Plunkett S, Liebscher GE, McCorvy JD, Bräuner-Osborne H, and Kristensen JL (2015) Synthesis and pharmacological evaluation of *N*-benzyl substituted 4-bromo-2,5-dimethoxyphenethylamines as 5-$HT_{2A/2C}$ partial agonists. *Bioorg Med Chem* **23**:3933–3937.

Harmon JL, Wills LP, McOmish CE, Demireva EY, Gingrich JA, Beeson CC, and Schnellmann RG (2016) 5-HT_2 receptor regulation of mitochondrial genes: unexpected pharmacological effects of agonists and antagonists. *J Pharmacol Exp Ther* **357**:1–9.

Hendricks PS, Clark CB, Johnson MW, Fontaine KR, and Cropsey KL (2014) Hallucinogen use predicts reduced recidivism among substance-involved offenders under community corrections supervision. *J Psychopharmacol* **28**:62–66.

Herth MM, Petersen IN, Hansen HD, Hansen M, Ettrup A, Jensen AA, Lehel S, Dyssegaard A, Gillings N, Knudsen GM, and Kristensen JL (2016) Synthesis and evaluation of (18)F-labeled 5-HT2A receptor agonists as PET ligands. *Nucl Med Biol* **43**:455–462.

Hjorth SA, Thirstrup K, and Schwartz TW (1996) Radioligand-dependent discrepancy in agonist affinities enhanced by mutations in the kappa-opioid receptor. *Mol Pharmacol* **50**:977–984.

Jensen AA, Plath N, Pedersen MH, Isberg V, Krall J, Wellendorph P, Stensbøl TB, Gloriam DE, Krogsgaard-Larsen P, and Frølund B (2013) Design, synthesis, and pharmacological characterization of *N*- and *O*-substituted 5,6,7,8-tetrahydro-4H-isoxazolo[4,5-d]azepin-3-ol analogues: novel 5-HT_{2A}/5-HT_{2C} receptor agonists with pro-cognitive properties. *J Med Chem* **56**:1211–1227.

Johnson MW, Garcia-Romeu A, Cosimano MP, and Griffiths RR (2014) Pilot study of the 5-HT_{2A}R agonist psilocybin in the treatment of tobacco addiction. *J Psychopharmacol* **28**:983–992.

Juncosa JI, Jr, Hansen M, Bonner LA, Cueva JP, Maglathlin R, McCorvy JD, Marona-Lewicka D, Lill MA, and Nichols DE (2013) Extensive rigid analogue design maps the binding conformation of potent *N*-benzylphenethylamine 5-HT_{2A} serotonin receptor agonist ligands. *ACS Chem Neurosci* **4**:96–109.

Kenakin T, Watson C, Muniz-Medina V, Christopoulos A, and Novick S (2012) A simple method for quantifying functional selectivity and agonist bias. *ACS Chem Neurosci* **3**:193–203.

Kenakin TP (2017) *Pharmacology in Drug Discovery and Development; Understanding Drug Response*, pp 56–58, Elsevier/Academic Press, Cambridge, MA

Keov P, Sexton PM, and Christopoulos A (2011) Allosteric modulation of G protein-coupled receptors: a pharmacological perspective. *Neuropharmacology* **60**:24–35.

Kometer M, Schmidt A, Bachmann R, Studerus E, Seifritz E, and Vollenweider FX (2012) Psilocybin biases facial recognition, goal-directed behavior, and mood state toward positive relative to negative emotions through different serotonergic subreceptors. *Biol Psychiatry* **72**:898–906.

Leth-Petersen S, Bundgaard C, Hansen M, Carnerup MA, Kehler J, and Kristensen JL (2014) Correlating the metabolic stability of psychedelic 5-HT_{2A} agonists with anecdotal reports of human oral bioavailability. *Neurochem Res* **39**:2018–2023.

Maroteaux L, Ayme-Dietrich E, Aubertin-Kirch G, Banas S, Quentin E, Lawson R, and Monassier L (2017) New therapeutic opportunities for 5-HT_2 receptor ligands. *Pharmacol Ther* **170**:14–36.

McCorvy JD and Roth BL (2015) Structure and function of serotonin G protein-coupled receptors. *Pharmacol Ther* **150**:129–142.

Meltzer HY (2012) Serotonergic mechanisms as targets for existing and novel antipsychotics. *Handb Exp Pharmacol* **212**:87–124.

Millan MJ, Marin P, Bockaert J, and Mannoury la Cour C (2008) Signaling at G-protein-coupled serotonin receptors: recent advances and future research directions. *Trends Pharmacol Sci* **29**:454–464.

Nau F, Jr, Miller J, Saravia J, Ahlert T, Yu B, Happel KI, Cormier SA, and Nichols CD (2015) Serotonin 5-HT_2 receptor activation prevents allergic asthma in a mouse model. *Am J Physiol Lung Cell Mol Physiol* **308**:L191–L198.

Nau F, Jr, Yu B, Martin D, and Nichols CD (2013) Serotonin 5-HT_{2A} receptor activation blocks TNF-α mediated inflammation in vivo. *PLoS One* **8**:e75426.

Nelson DL, Lucaites VL, Wainscott DB, and Glennon RA (1999) Comparisons of hallucinogenic phenylisopropylamine binding affinities at cloned human 5-HT_{2A}, -HT_{2B} and 5-HT_{2C} receptors. *Naunyn Schmiedebergs Arch Pharmacol* **359**:1–6.

Nichols DE (2016) Psychedelics. *Pharmacol Rev* **68**:264–355.

Nichols DE, Johnson MW, and Nichols CD (2017) Psychedelics as medicines: an emerging new paradigm. *Clin Pharmacol Ther* **101**:209–219.

Nørskov-Lauritsen L, Thomsen AR, and Bräuner-Osborne H (2014) G protein-coupled receptor signaling analysis using homogenous time-resolved Förster resonance energy transfer (HTRF®) technology. *Int J Mol Sci* **15**:2554–2572.

Persson M, Løye AF, Mow T, and Hornberg JJ (2013) A high content screening assay to predict human drug-induced liver injury during drug discovery. *J Pharmacol Toxicol Methods* **68**:302–313.

Pigott A, Frescas S, McCorvy JD, Huang XP, Roth BL, and Nichols DE (2012) *trans*-2-(2,5-Dimethoxy-4-iodophenyl)cyclopropylamine and *trans*-2-(2,5-dimethoxy-4-bromophenyl)cyclopropylamine as potent agonists for the 5-HT_2 receptor family. *Beilstein J Org Chem* **8**:1705–1709.

Redrobe JP, Jørgensen M, Christoffersen CT, Montezinho LP, Bastlund JF, Carnerup M, Bundgaard C, Lerdrup L, and Plath N (2014) In vitro and in vivo characterisation of Lu AF64280, a novel, brain penetrant phosphodiesterase (PDE) 2A inhibitor: potential relevance to cognitive deficits in schizophrenia. *Psychopharmacology (Berl)* **231**:3151–3167.

Rickli A, Luethi D, Reinisch J, Buchy D, Hoener MC, and Liechti ME (2015) Receptor interaction profiles of novel *N*-2-methoxybenzyl (NBOMe) derivatives of 2,5-dimethoxy-substituted phenethylamines (2C drugs). *Neuropharmacology* **99**: 546–553.

Risgaard R, Ettrup A, Balle T, Dyssegaard A, Hansen HD, Lehel S, Madsen J, Pedersen H, Püschl A, Badolo L, et al. (2013) Radiolabelling and PET brain imaging of the α_1-adrenoceptor antagonist Lu AE43936. *Nucl Med Biol* **40**:135–140.

Rosenkilde MM, Cahir M, Gether U, Hjorth SA, and Schwartz TW (1994) Mutations along transmembrane segment II of the NK-1 receptor affect substance P competition with non-peptide antagonists but not substance P binding. *J Biol Chem* **269**: 28160–28164.

Rosenkilde MM and Schwartz TW (2000) Potency of ligands correlates with affinity measured against agonist and inverse agonists but not against neutral ligand in constitutively active chemokine receptor. *Mol Pharmacol* **57**:602–609.

Roth BL (2011) Irving Page Lecture: 5-HT_{2A} serotonin receptor biology: interacting proteins, kinases and paradoxical regulation. *Neuropharmacology* **61**:348–354.

Sagan S, Beaujouan JC, Torrens Y, Saffroy M, Chassaing G, Glowinski J, and Lavielle S (1997) High affinity binding of [3H]propionyl-[Met(O_2)11]substance P(7–11), a tritiated septide-like peptide, in Chinese hamster ovary cells expressing human neurokinin-1 receptors and in rat submandibular glands. *Mol Pharmacol* **52**:120–127.

Schmid Y, Enzler F, Gasser P, Grouzmann E, Preller KH, Vollenweider FX, Brenneisen R, Müller F, Borgwardt S, and Liechti ME (2015) Acute effects of lysergic acid diethylamide in healthy subjects. *Biol Psychiatry* **78**:544–553.

Sewell RA, Halpern JH, and Pope HG, Jr (2006) Response of cluster headache to psilocybin and LSD. *Neurology* **66**:1920–1922.

Sleight AJ, Stam NJ, Mutel V, and Vanderheyden PM (1996) Radiolabelling of the human 5-HT_{2A} receptor with an agonist, a partial agonist and an antagonist: effects on apparent agonist affinities. *Biochem Pharmacol* **51**:71–76.

Yu B, Becnel J, Zerfaoui M, Rohatgi R, Boulares AH, and Nichols CD (2008) Serotonin 5-hydroxytryptamine$_{2A}$ receptor activation suppresses tumor necrosis factor-α-induced inflammation with extraordinary potency. *J Pharmacol Exp Ther* **327**: 316–323.

Zhang G and Stackman RW, Jr (2015) The role of serotonin 5-HT_{2A} receptors in memory and cognition. *Front Pharmacol* **6**:225.

Address correspondence to: Jesper Langgaard Kristensen, Department of Drug Design and Pharmacology, Faculty of Health and Medical Sciences, Universitetsparken 2, 2100 København Ø, University of Copenhagen, Denmark. Phone: +45 35 33 64 87, E-mail: jesper.kristensen@sund.ku.dk